BOOK: 2D Materials for Water Purification
Editor: Rasel Das

CHAPTER:
Molybdenum and Tungsten Disulfide as Novel Two-dimensional Nanomaterials in Separation Science

Mateus H. Köhler[†], João P. K. Abal[‡], Gabriel V. Soares[‡] and Marcia C. Barbosa[‡]

[†]Department of Physics, Federal University of Santa Maria, 97105-900, Santa Maria, Brazil

[‡]Institute of Physics, Federal University of Rio Grande do Sul, 91501-970, Porto Alegre, Brazil

Abstract

Beyond graphene-based membranes for water desalination a vast horizon of new materials has been discovered for solutes separation from water. In this realm, the transition-metal dichalcogenides (TMDs) molybdenum and tungsten disulfide (MoS_2 and WS_2, respectively) stand as promising two-dimensional (2D) materials. Their tailoring for nanofluidics as well as the emerging synthesis and production methods unfold the possibility of applying MoS_2 and WS_2 in modern desalination processes based on 2D membranes. We present here an overview from their theoretical conception to their state-of-the-art applications, highlighting the challenges and opportunities associated with measuring water flow and ionic rejection rates at nanoscale. In a world full of environmental concerns, both the theoretical gaps and experimental perspectives point toward a promising use of MoS_2 and WS_2 as green components in separation technologies, contributing to increase the availability of clean, potable water.

7.1. Introduction

Since the very beginning of this century we have witnessed a race to shrink the dimensions of fluidic devices to the nanometer scale. The use of nanotubes or nanopores made new discoveries on fluid transport possible, putting even classical hydrodynamics in check [1]. In fact, two-dimensional (2D) materials were not even considered beyond the desks of physicists and chemists until quite recently with the rise of graphene, a one-carbon-atom-thick structure. The discovery of this fascinating material and its exceptional properties [2, 3] completely changed the game.

While much research is still focused on carbon nanotubes (CNTs) [4], zeolites [5], polymers [6] or ceramics [7] to act as membranes for ion separation, the fact is that graphene and graphene-related materials have taken over the news with promising nanofiltration results. More recently, van der Waals (vdW) assembly of 2D materials has been used to create artificial channels with sub-nanometer-scale precision [8]. Two of these vdW structures,

molybdenum disulfide (MoS_2) and tungsten disulfide (WS_2), stand as prominent alternatives to graphene, exhibiting many similar characteristics as atomic thickness, large surface area, mechanical strength, extreme durability, and also the most important: an exotic love-hate relationship with water that leads to high permeation rates. MoS_2 is the most widely employed TMD in a range of applications and has recently been investigated for its potential in separation techniques. This prototypical TMD is made up of a middle layer of molybdenum sandwiched between two sulfur layers with thickness of ∼1 nm and a robust Young's modulus of ∼300 GPa [9] (comparable to the Young's modulus of steel). TMDs, a family of over 40 materials, are represented by the generalized formula MX_2 and consist of a transition metal (M), for example, Mo, W or Ni packed between two chalcogens (X) such as S, Se or Te. The coordination of a transition metal by chalcogens in a TMD structure opens up the possibility for multiple stacking sequences. As illustrated in Figure 7.1, a single-layered TMD generally presents either an octahedral or a trigonal prismatic coordination phase. In multi-layered TMDs, a large variety of polymorphic structures arise as each individual layer can possess any of the two coordination phases. The three commonly found polymorphs are defined as 1T, 2H and 3R, where the digit is indicative of the number of layers in the crystallographic unit cell, and the letter designates the symmetry: T for tetragonal (D_{3d} group), H for hexagonal (D_{3h} group), and R for rhombohedral (C^5_{3v} group). The 1T form displays metallic behavior, while both 2H and 3R forms exhibit semi-conducting behavior. Each TMD polymorph possesses unique structural and electronic properties, which can be further explored to build efficient adsorbent devices and desalination membranes.

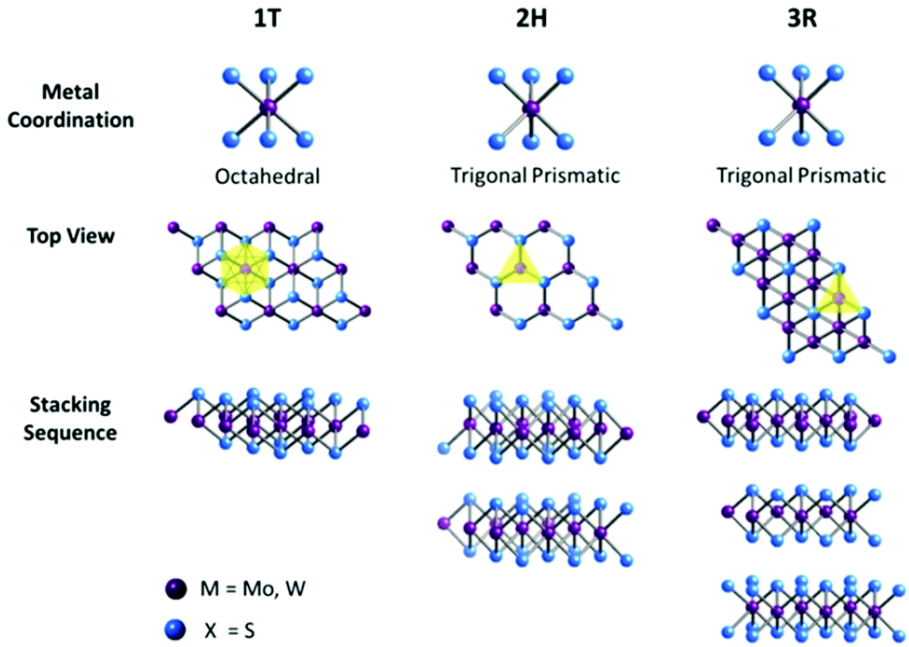

Figure 7.1: Illustration of metal coordinations and stacking sequences of TMD structural unit cells. Adapted with permission from Toh et al. [10].

Recent works have reported high water permeability and selectivity of MoS_2 nanosheets, both desired features in desalination membranes. A flexible laminar separation membrane prepared from MoS_2 sheets exhibited a water flux from 3 to 5 times higher than that reported for graphene oxide (GO) and rejected 89 and 98% of evans blue and cytochrome C molecules, respectively [11]. The possibility to craft the pore edge with Mo, S or both provides flexibility to design nanopores within the membrane with the desired functionality. Another option

for creating a desalination membrane is to use stacking layers of MoS_2 instead of crafting a pore. A few-layer MoS_2 membrane of only 7 nm thick, grown by Chemical Vapor Deposition (CVD) technique, has allowed for an excellent combination of high water permeability (> 322 $L{\cdot}m^{-2}{\cdot}h^{-1}{\cdot}bar^{-1}$) and high ionic sieving capability ($> 99\%$) for various seawater salts including Na^+, K^+, Ca^{2+}, and Mg^{2+} with a range of concentrations [12]. Near 100% of salt ion rejection rates for actual seawater obtained from the Atlantic coast was also reported, significantly outperforming the previously developed 2D MoS_2 layer membranes of micrometer thickness as well as conventional reverse osmosis (RO) membranes. These results confirmed previous theoretical and computational predictions about desalination capacity and water permeation of 2D nanoporous MoS_2 [13, 14].

Advancing the search for high-performance lamellar separation membranes, Sun et al. [15] investigated the potential of WS_2, a semiconductor material similar to MoS_2, with a Young's modulus of $\sim$270 GPa [16]. The bulk structure was exfoliated and a thin film was constructed via filtration. The lamellar WS_2 membrane exhibited water flux five times greater than GO membranes and two times greater than MoS_2 laminar membranes, rejecting 90% of evans blue molecules. This impressive water permeance further increased from 450 to 930 $L{\cdot}m^{-2}{\cdot}h^{-1}{\cdot}bar^{-1}$ with the addition of metal hydroxide nanostrands. They created additional channels between the WS_2 layers allowing for increased water transport without degrading the membrane's salt rejection properties.

Understanding the mechanisms and peculiarities of 2D membrane-based desalination is the ultimate frontier to reach industrial scale. So far, cutting-edge theoretical work has been driving advances and pointing directions for experimental work with some success. But we still need more. We need to merge theoretical advances with new experimental approaches, such as the scalable method to controllably make nanopores in single-layer TMDs or nanoscale water velocity profile mapping introduced by Secchi and collaborators [17], always sharing the goal of making large scale application of MoS_2 and WS_2 membranes in water purification possible. It is important to note that in terms of using nanostructured membranes in desalination technology, such as RO systems, these advances open the door to work with a new paradigm of membrane permeability and selectivity.

7.2. Computer Simulations

Before computers took over every laboratory − and even our daily life − science was based on the assumption that we could only model the natural world through the lenses of experiments and purely theoretical works. Take the example of the Dutch: they built the Netherlands as we know it today with the help of the Delta Works, a set of megastructures that hold back the ocean. To put together this enormous project they had to build the Waterloopkundig Laboratorium, a massive concrete-based hydrological laboratory conceived after World War II, in the pre-computer age, where water could be guided into and out of large-scale trial models. Contemporarily it is almost impossible to think of a world where things, from a small pen to a huge hydroelectric plant, are not designed on a computer.

During an experiment, a set of results can be obtained directly from measuring the properties of a system. Alternatively, a mathematical description could be used to create a model, which in turn can be validated by its ability to describe some physical behavior. Today, we have another tool to probe a physical system: computer simulations. A model is provided by theorists but the calculations can be carried by machines following some recipe. In this way, computer simulations unlocked the possibility to study more complex and realistic systems, becoming a bridge between theoretical models and real world experiments [18].

There is no doubt that computer simulations play an important role in contemporary science development. Several different computational approaches can be used to study physical systems. For example, when we aim to investigate nanoscaled structures the interactions between atoms are the core of the simulation. Often, empirical interatomic potentials (as Lennard-Jones potentials) are fitted to reproduce a given experimental property using van der Waals systems as basis. Thereby, molecular dynamics (MD) simulations are used to obtain the temporal evolution of different systems. But if the interest resides on the electronic structure of a strongly covalent material, electronic correlations are very important and we need to use *ab initio* methods such as density functional theory (DFT). We can even merge both approaches and use DFT to parameterize Lennard-Jones potentials that will be further used in MD simulations. Method suitability will depend on which kind of properties we are interested in, from infrared spectra to dynamical and thermodynamical information.

Just like a puzzle that fits piece by piece, MD simulations adapted perfectly to the study of physical and chemical properties of nanofluidic systems. They have allowed us to probe a wide range of microscopic behaviors that otherwise would be tremendously difficult to access at nanoscale. Simulations within MD machinery are usually performed in a feasible timescale with high accuracy. In other words, the MD approach is the mechanism in which we can perform computational simulations that take into account thermodynamic and dynamic behaviors of nanofluidic systems. It means that this approach can be viewed as a bridge between the quantum realm (hidden in atomic interactions and sizes) and classical hydrodynamics.

While there are clear benefits in using MD simulations, there are also major challenges. Computational materials scientists have worked hard to design general, accurate and reliable molecular and atomistic models. For example: in the case of water, the model chosen to represent atomic geometries and interaction parameters is the seed in which the whole dynamic relies on, so that the physics can emerge following the classical equations of motion. The mainstream model in MD simulations is based on the Lennard-Jones potential plus a Coulombic term. The task of finding the right model − which is generally suitable only for a handful of specific systems− has haunted theoretical physicists and chemists since the first computer simulation of liquid water with the Bernal-Fowler model in 1969. Even with the help of new experimental data and theories being developed, water is still notoriously hard to model and remains relatively poorly understood, with several anomalous properties − behaviors which contradict general theories on the liquid state of matter.

The interest in nanometric desalination systems has led us to question how the key properties of saline solutions can be captured in a computer simulation (e.g. mixing different interaction parameters). One of the most widely used methodology to classically simulate salt water desalination consists in creating a box with the membrane located between two reservoirs, each one pressed by a piston − usually graphene-made. This imposes a controlled pressure gradient in water as illustrated in Figure 7.2(a). Here we can highlight that (*i*) as we apply different pressures in each reservoir and (*ii*) the solutions are at different concentrations, the system is not under thermodynamic equilibrium. In fact, these simulations aim to find water transport and salt rejection rates acquired at a steady-state flow, which is only possible in non-equilibrium states. Of course that as the simulation runs the system will eventually reach equilibrium. But to mimic an actual nanoscaled RO scenario the simulation should be far from this point.

In order to filter water using 2D membranes, we can use either the interlayer spacing, forcing water to flow through the structure gaps, or drill holes (nanopores) in the membrane. In any case, it is important to ensure that the nanopore size allows only for the flow of water molecules. Interestingly, nanopores in 2D materials such as TMDs will naturally appear during the growth process. Point defects, grain boundaries and van der Waals (vdW) gaps, among other structural

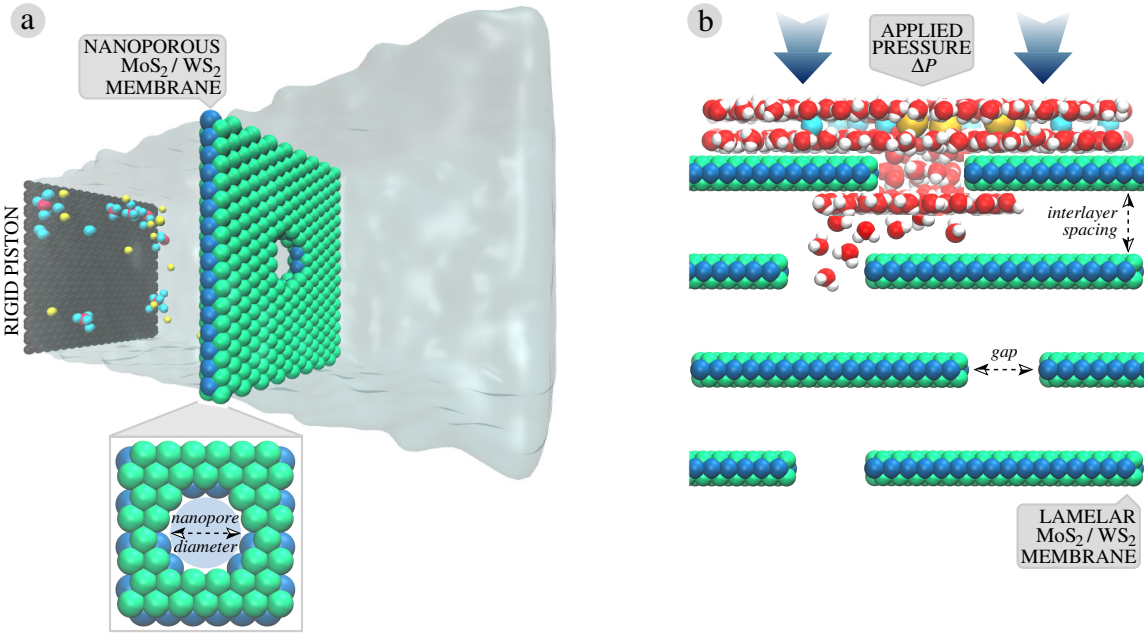

Figure 7.2: Archetypal systems used in computer simulations of water desalination with (a) nanoporous and (b) lamellar MoS_2 and WS_2 membranes.

deformations, have been observed in CVD grown of MoS_2 and WS_2 monolayers [19, 20, 21]. At first glance this might seem like a disadvantage, but the truth is that these "flaws" lead to the emergence of nanopores and nanogaps that can be used to desalinate water and remove heavy metals, biomolecules and other pollutants. In the case of MoS_2, for instance, these intrinsic defects appear in high concentrations ($\sim 10^{13}$ cm^{-2} for sulfur vacancies [22]). However, these "natural" pores are randomly distributed with varied sizes, which pose a challenge for scalability – a very important aspect in large-scale production.

MoS_2 and WS_2 nanoporous membranes were idealized by theoretical calculations based on MD simulations, which predicted superior desalination performances. While simulations involving MoS_2 interaction potentials have been more frequent, results for WS_2 are more scarce due to the lack of proper force fields. There are frictional losses in these systems that dominate fluid transport, and this phenomenon is mostly related to the nanopore's entrance. MD simulations have shown that in this region, water flux is intrinsically connected with a complex hydrogen bonding (HB) network and the ability to enter the nanopore is governed by a combination of favorable geometric orientations and HB configurations [23]. Interestingly, water flux scales linearly with pore area when there is a big enough pore size [24]. For smaller pores, a nonlinear relationship between water transport and pore area appears, which implies that the phenomenon cannot be explained based on classical hydrodynamics (continuum fluid model). This happens when the water-membrane terms acquire higher importance than the HB network interaction, which is a result of a reasonable fraction of total confined water interacting with the wall – something that does not occur with bigger pores.

We could think of the desalination process through 2D membranes as a collection of small events, all happening at the same time. We could thus highlight the main mechanisms as: size exclusion, steric exclusion of the hydration shell, charge repulsion (pore chemistry), nanopore morphology, complex solute-pore interactions and entropy gradients. The first is directly related with ion/nanopore size ratio, and the second comes from the fact that these ions in water are surrounded by a hydration shell, which means that in order to enter the nanopore the ions need to bare themselves from the water shell at some energy penalty. Both the pore's chemistry and

morphology are going to affect possible HB configurations, that results in an impact to salt permeation. The fifth mechanism can be viewed as the possibility of mixing different ions and observing different salts rejection. At last, entropic differences can be expressed as a mix of nanopore morphology, charge distribution and so on as a result of the possible configurational restrictions, which in turn affects the free energy barrier through the membrane.

When it comes to cleaning aqueous solutions using membranes, we need to face a range of ions with different valences. Fortunately, MD simulations on solutions of water and three cations with different valences (Na^+, Zn^{2+} and Fe^{3+}) indicate that the higher the valence, the greater the ion rejection through 2D nanoporous MoS_2 and graphene [13]. The desalination rates were confirmed even under a wide range of test conditions, including high pressures and different nanopore sizes.

The cation charge dependence leads to another question: what if we add more cations with higher valence to the solution? It would seem very inappropriate at first, but surprisingly, simulations have shown that this procedure can lead to higher desalination rates [25]. The possible reason is that the whole membrane-mediated desalination process is based on the assumption that size matters. Furthermore, the combination of larger ions and smaller nanopores (large enough to let water pass) is crucial for an efficient selectivity. When high valence ions are added, they aggregate with counterions to form clusters that in time will be rejected by the membrane.

There are physical and chemical aspects that can be decisive either to improve or to hinder 2D-membrane-based desalination. Unfortunately, very few experimental studies of ionic conductance through MoS_2 and WS_2 nanoporous membranes with diameters lower than 2.0 nm have been reported. Almost all of our knowledge is based on computational simulations and theoretical models. For instance, one important parameter to control the flow through the nanopore is ionic conductance. Perez et al. [26] developed a continuum model of ionic conductivity for a KCl electrolyte through a sub 5-nm single-layer MoS_2 nanopore using equilibrium all-atom MD simulations. They showed that electrolyte behavior deviates by 50% from bulk properties for diameters below 2.0 nm: ion pore conductivity is about half of the bulk value for 2.0 nm and only a third when the diameter approaches 1.0 nm. Their results corroborate the idea that the nanopore's size plays a fundamental role in the desalination process.

Usually, layer-stacked membranes made of 2D MoS_2 and WS_2 are synthesized with hundreds to thousands of nanosheets. But this thickness is unlikely to be modeled in a traditional MD simulation due to computational limitations. Alternatively, we can take advantage of the fact that there is a relation between measured flux and membrane thickness. Indeed, if we fit the water flux versus the membrane thickness we can get a parabolic dependence in a way that we can estimate the experimental value. For instance, Wang et al. [27] noticed that the predicted flux decreases as membrane thickness increases, consistent with their experimental data. They found that as their model membrane thickness increased to $\sim$500 nm, water flux would decrease to around 50 $L{\cdot}m^{-2}{\cdot}h^{-1}{\cdot}bar^{-1}$, matching the experimental value.

Whether measuring mass transport properties or the membrane's mechanical strength, computer simulations have constantly contributed to the prediction and confirmation of 2D membranes' use for desalination. There are many aspects which can make a certain material a good candidate to be used in desalination membranes. High structural strength when subjected to high pressures is certainly one of them. Therefore, as important as the ability to retain ions is the membrane's ability to remain stable under strong external pressures. Unfortunately, an experimental work by Sun et al. [15] showed that nanochannels created in lamellar thin films of WS_2 with the addition of metal hydroxide nanostrands can crack under high pressure. Although first-principles calculations revealed a Young's modulus $Y = 200$ GPa for 2D WS_2,

comparable to stainless steel, finite-element-based mechanical simulations confirmed the collapse of cylindrical channels at a critical pressure of ∼1.6 GPa. All of these structural fractures could pose a significant problem regarding the membrane's desalination capacity. Remarkably, the formation of nano-cracks within the WS_2 membrane was found to increase water permeance as a consequence of increased porosity. In other words, the crack produces new fluidic nanochannels that further results in water fluxes 4 times higher than that of the as-prepared WS_2 membrane, without rejection performance degradation. According to Sun's group, these membranes have separation performances 2 orders of magnitude higher than that of commercial membranes with similar rejection rates.

7.3. MoS_2 and WS_2 Syntheses and New Fabrication Methods

Usually 2D materials are the basic building blocks of bulk materials when they are stacked together layer-by-layer. The possibility to obtain a single layer of carbon (graphene) from bulk graphite has led to exciting new physics and material properties, for instance: atomically thin electrical and thermal conductors, high transparency to visible light and a high carrier mobility [28]. After the first works on graphene isolation by micromechanical exfoliation, several other methods to obtain graphene were investigated, such as molecular beam epitaxy [29], CVD on metal surfaces [30], and graphene films on silicon carbide (SiC) single crystals formed by silicon evaporation [31], among others. Yet, none of these growth methods completely fulfills every basic requirements for applications where suitable size and quality are mandatory, such as in high performance electronic devices. Still, some of this growth methods such as CVD and silicon evaporation from SiC crystals can be used in applications with less restricted requirements, namely: anti-corrosion coatings and paints [32], nanoporous membranes for desalination [33], and pesticide biosensing [34]. Moreover, the electronic band structure of graphene has a linear dispersion near the K point, where the bottom of the conduction band touches the top of the valence band, making it a zero gap semiconductor. This provides a great challenge to produce electronic devices for many applications where high 'on and off' electrical current ratios are required.

In the past decade many other 2D materials have been isolated and studied, such as hexagonal boron nitride (h-BN), silicene, phosphorene, and TMDs. TMDs are a class of materials composed of a transition metal from groups IV to VI (such as Ti, Nb, W, Mo etc.) and a chalcogen (S, Se or Te). Different from graphene, these 2D materials are composed of three layers of atoms, where a metal plane is bonded to a chalcogen plane on both sides. They usually present a hexagonal crystal structure, where the wide range of possible compositions leads to several distinct optical, electrical and mechanical properties. For instance, TMDs can present metallic ($NbTe_2$, $TaTe_2$) and superconducting [35] (NbS_2, TaS_2) or semiconducting [36] (MoS_2, WS_2) electronic properties. Interestingly, TMDs' properties have some degree of reliance upon the number of layers, where the chalcogen-metal-chalcogen structure is considered a monolayer. One of the most common properties dependent on the number of layers is the TMDs' band structure. Many of them present a transition from an indirect (bulk material) to a direct (monolayer) band gap, allowing for optoelectronic devices application[37]. One example is the MoS_2 transition from bulk with a 1.3 eV indirect band gap to a 1.8 eV direct band gap in monolayer form [38]. A similar effect is also observed in graphene when it presents a band gap different from zero [39] or superconductivity [40] in a bilayer structure.

The reproducible synthesis of 2D materials is mandatory for characterizing these layer prop-

erties, as well as providing a path for their integration into a variety of applications. It is possible to distinguish between two most widely used methods to synthesize single- and few-layer 2D materials: the top-down and bottom-up methods. The first is based on the exfoliation of layered bulk van der Walls crystals, while the latter is obtained by CVD growth on different substrates. The micromechanical exfoliation has been used routinely to obtain 2D flakes, which may contain from several crystal layers to a single monolayer. Van der Walls crystalline solids are usually employed as the base material for exfoliation. The crystal structure is composed of atom layers strongly bonded covalently or ionically in-plane, and these planes are staked together by weak van der Walls forces. These van der Walls energies are in the range of few of meV, which enable the easy exfoliation of the atomic layers. This was the approach used to obtain the first graphene layers [2] and it is still used for a wide range of materials, predominantly using a tape as the (dry) exfoliation method. 2D materials such as MoS_2, black phosphorus [41], and h-BN [42] have been obtained using this procedure. The obtained 2D monolayers present the same crystal structure as their bulk counterparts, and can remain thermodynamically stable under ambient conditions up until weeks. This method of isolation of individual and few layers still is one of the most widely used to study their properties and for the fabrication of electronic devices, since it can produce monolayers with high quality. Nevertheless, it is mostly limited to crystal sizes in the order of some μm, making it unsuitable for large area applications.

Conversely, CVD growth is able to produce high quality 2D materials with controlled size, number of layers and superior electronic properties. Specifically, this method has been used to produce large-area MoS_2, WS_2, graphene and h-BN, which can be integrated in the fabrication of nanoelectronic devices.

MoS_2 growth can be obtained using two different precursors, one that contains Mo and another that contains sulfur. The process involves typically MoO_3 and S powders, where the substrate can be a dielectric (such as SiO_2) or conductor (graphene), among others. It consists in heating MoO_3 to become volatile as some sub-oxide (MoO_x), and then reacts with the sulfur vapor to produce MoS_2 of the desirable substrate. There are many variations of this process that can lead to MoS_2 layers with sizes up to a few mm. In some cases, the MoO_3 is first deposited on the substrate and then it is submitted to the sulfur vapor annealing. Some works have reported on the deposition of Mo films that were later sulfurized to produce MoS_2 [43]. Modulating the homogeneity and thickness of Mo and/or MoO_3 film determines the quality and thickness of the MoS_2 film. In any case, this CVD approach has been shown to be highly scalable.

In some cases, a single precursor which contains both elements has been used [44]. $(NH_4)_2MoS_4$ can be thermally decomposed on insulating substrates and, similarly to the process described above, can also yield large-area MoS_2 in the presence of sulfur vapor. Moreover, transistors based on this CVD-prepared MoS_2 showed good electronic properties with large on/off ratios [45]. Nevertheless, these values are lower than those obtained from the mechanically exfoliated MoS_2, because the crystal defects shown in the CVD-grown films can be deleterious to carrier mobility [46]. Finally, recent works on a variation of CVD, the metal-organic (MO)CVD using bis(tert-butylimido)-bis(dimenthylamido)molybdenum and dietyl disulfide have produced MoS_2 layers from 1 to 25 nm thick at short deposition times (90 s) and with great uniformity on 50 mm SiO_2/Si wafers [47], making it very promising for large-scale applications.

WS_2 posses similar electrical, mechanical and optical properties as MoS_2 and can be synthesized in a similar fashion. For instance, the band structure of WS_2 is also dependent on the number of layers since bulk WS_2 is a semiconductor with indirect band gap of 1.4 eV, while monolayer WS_2 presents a direct band gap of 2.1 eV [48]. It is also possible to obtain WS_2 through micromechanical exfoliation and CVD. Dry exfoliation is very similar as in the

case of graphene and MoS_2: a tape is applied to a bulk WS_2 crystal removing from single to few-layers of WS_2 which can be transferred on the desirable substrate. Superior crystal and electronic properties are obtained using this method, but it lacks on scalability. Chemical (wet) exfoliation has also been reported [49].

The W-based precursors for CVD growth of WS_2 present higher melting points than the ones used in the MoS_2 growth. For instance, W has a melting point of 3422°C and WO_3 of 1473°C [43]. This makes WS_2 deposition more challenging than MoS_2, since the Mo-precursors present a lower melting point. Still, the basic approach is similar for both materials: reaction of sulfur vapor with a W-precursor at high temperatures, which is deposited on the substrate.

The most common precursors are WO_3 and sulfur powder. They are heated inside a reactor under an inert gas flow, such as argon. The reactor temperature is usually in the 850-950°C range. Among the challenges also observed in the growth of MoS_2 (homogeneity, crystal quality, mechanical and electrical properties, layer number control, etc), one of the main issues for WS_2 growth is the high temperatures employed in its process. In this manner, there is a limitation on the type of substrate that can be used to grow WS_2. Some works have reported on the use of alternative W-precursors in order to lower growth temperature, such as the use of WCl_6 [50]. A great effort must be made in order to grow WS_2 directly on several types of substrates and materials.

7.4. Feasibility of Free-Standing MoS_2 and WS_2 Membranes in Filtration

Recently, free-standing membranes of 2D materials have attracted attention due to their wide range of application, including piezoelectricity in MoS_2 [51], single-molecule DNA sensing [52], high Young modulus [9] and water desalination [11, 53]. They can also be used to investigate fundamental properties of 2D materials, since free-standing membranes are not influenced by underlying substrates [54, 55, 56].

Free-standing WS_2 membranes have also been produced using similar methods. The most used approach to produce these membranes is to use a substrate containing an array of circular or square holes, usually produced by chemical or e-beam lithography. After that, the desirable 2D material (MoS_2 or WS_2) is transferred to this substrate's surface. Since the transference process of CVD 2D materials can be difficult, the use of exfoliated materials is preferred.

Eda et al. [57] have prepared MoS_2 nanosheets by chemical exfoliation using organolithium intercalation and forced hydration. Li intercalates between MoS_2 layers, and when it reacts with water, it increases the plane spacing with hydrogen gas. The resulting MoS_2 is then used to produce layer-stacked membranes. Using a CVD approach, Waduge et al. [56] prepared micrometer scale apertures in silicon nitride membranes, which were placed above a boat containing MoO_2. A second boat containing sulfur was heated and the carrier gas (Ar) transported the sulfur vapor to the silicon nitride membranes. The growth process takes place at 750°C leading to selective MoS_2 growth near the apertures.

7.4.1. MoS_2 and WS_2 Membranes Compared to Other 1D/2D Materials

One of the most interesting discoveries of our time and hypothesized as fruitful for a large range of future technological applications is the role of dimensionality in determining the properties of a material. Ultrathin 2D nanosheets of layered TMDs are fundamentally intriguing.

Aside from presenting electronic properties diverse from the bulk, this group of materials exhibits versatile chemistry in contrast with graphene's chemically inert behavior [35]. Furthermore, 1D materials have attracted a lot of attention once theoretical and experimental observations led to the discovery of anomalous water transport under certain conditions, enabling nanofluidic flow enhancement in CNTs [58]. In this section, the MoS_2 and WS_2 membranes will be compared to other 1D/2D materials from the computational and experimental perspective.

A general 2D material can be used to transform a very thick membrane into two kinds of construction design: a nanoporous membrane or a layer-stacked membrane [59]. In terms of desalination purposes, nanoporous membranes of MoS_2 and WS_2 are very peculiar for they present a mix of hydrophobic and hydrophilic edges, which in turn can be tuned to enhance water permeability and salt rejection. Heiranian et al. [14] constructed nanoporous membranes with three pore edge types: the first labeled as *mixed* (a combination of molybdenum and sulfur atoms), and the other two labeled as *Mo only* and *S only* (terminated only by molybdenum or sulfur atoms, respectively). MD simulation analysis of water permeation through each membrane allowed them to conclude that *Mo only* pores and mixed pores perform better than *S only* pores regarding water flux. The reason is related to the fact that *Mo only* regions achieve higher local water density, hence attracting more water throughout all possible MoS_2 pore architectures. They applied the same methodology for different force-field parameters to mimic different membrane compounds, such as $MoSe_2$, $MoTe_2$, WS_2 and WSe_2 and reported that the transition metal atom plays a more important role than the chalcogen atom when it comes to choosing the best TMD material for desalination. Water permeability was found to be two to five orders of magnitude greater than in current technology and 70% better than graphene nanopore with similar sizes. These results demonstrate how the material's chemistry (especially in nanopores) leads to exotic relationships with water, which is attracted to the inner pore, enhancing both water permeation and rejection of unwanted substances.

Taking advantage of MoS_2 nanosheets imperfections, Li et al. [60] used MD simulations to propose a desalination process regulated by "open" and "closed" states induced by mechanical strain. By applying lateral strain to the MoS_2 membrane, they observed high water transport rate (355.3 $L{\cdot}m^{-2}{\cdot}h^{-1}{\cdot}bar^{-1}$) and excellent salt rejection capability when the membrane reached the open state, which corresponds to a strain of about 6% ($\sim$ 6% cross-sectional expansion in the membrane). The membrane demonstrated high water transparency and strong salt filtering capability even under a 12% strain. In this case, the mechanical strength associated with TMDs is a critical parameter, paving the way for a large-scale industrial application.

When it comes to the experimental realization of 2D MoS_2 membranes, the layer-stacked scheme is the current feasible option [59, 12, 61] due to the challenges concerning scalability and fabrication of large areas of MoS_2 monolayers [59] and the generation of nanopores with homogeneous size distribution. Nevertheless, 2D layer-stacked MoS_2 with few $\sim$7 nm thick layers has been recently tested with promising water permeability of up to 320 $L{\cdot}m^{-2}{\cdot}h^{-1}{\cdot}bar^{-1}$, and stable high ionic sieving capability ($>$ 99%) [12]. This type of membrane allows for water flow inbetween their grain boundaries and gaps. As for MoS_2, a 300 nm layer-stacked membrane of WS_2 exhibited even higher water permeance of 730 $L{\cdot}m^{-2}{\cdot}h^{-1}{\cdot}bar^{-1}$ [15] at the cost of rejecting 90% 3 nm evans blue molecules $-$ a typical solution procedure to evaluate rejection rates. In terms of RO saltwater purposes it is very important for a membrane to be able to reject 99.5% of salt at standard test conditions [62, 63].

To emulate the natural hydrophilicity present in both MoS_2 and WS_2 nanopores, it is possible to add chemical functional groups in nanoporous graphene to then adjust the pore's chemistry. Using classical MD simulations Cohen-Tanugi and Grossman [64] investigated water flux through hydrogenated (bonded with H) and hydroxylated (bonded with H and OH)

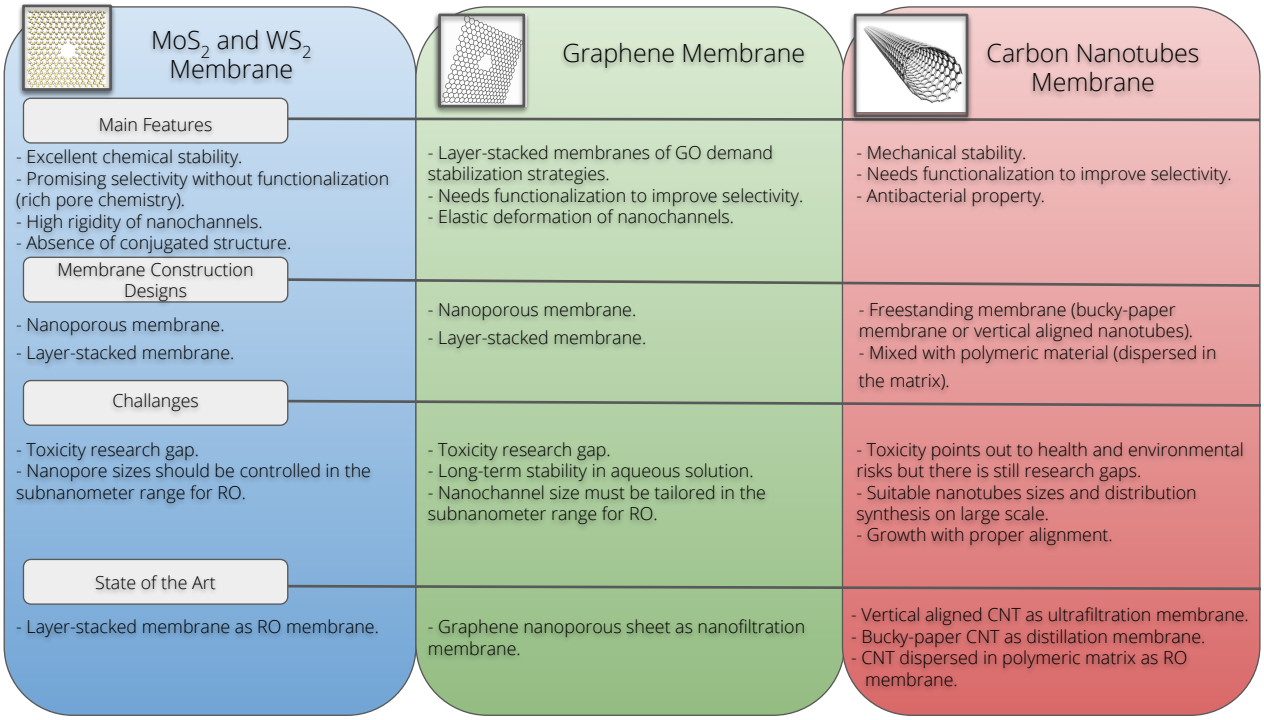

Figure 7.3: Comparison between MoS_2/WS_2 [59], graphene [66, 67, 68] and CNT membranes [69, 70, 71].

graphene nanopores. They reported permeabilities two to three orders of magnitude higher than commercial RO membranes at the same salt rejection rate for some nanopore sizes. By maintaining pore size and using hydroxyl groups they also discovered water flux enhancement when compared to the hydrogenated case. In addition, Risplendi et al. [65] used quantum (DFT) and classical (MD) simulations to show that functionalized graphene nanopores can reject even neutral solutes such as boric acid (H_3BO_3). In order to guide future membrane designs it is very important to understand the challenges involved in the commercialization of RO membranes such as chemical and thermal sensitivity, rapid fouling and cleaning.

An experimental work of Surwade et al. [72] demonstrated the possibility of using this kind of nanoporous graphene monolayer as a desalination membrane. The nanopores, produced through exposure to oxygen plasma, confirmed the indication of previous theoretical studies and presented a permeability of $\sim$252 $L{\cdot}m^{-2}{\cdot}h^{-1}{\cdot}bar^{-1}$ – assuming a nanopore density of 10^{12} cm^{-2} and sizes of 1 nm in diameter. Test conditions have further confirmed that graphene oxide membranes remain with excellent water permeance, separation efficiency, chemical and mechanical stability in water, acid and basic solutions even after months [73]. However, despite the attractive potential improvements in the manufacturing process, a cost-effective graphene-based desalination device and other 2D membranes is still uncertain. [66]

The option of layer-stacked graphene membranes is attractive comparing the industrial scale challenges related to the fabrication of large-area monolayer graphene with controlled pore density and size, a process which is intrinsically stochastic [67]. Although the water transport mechanism is a bit different in stacked graphene oxide (GO) nanosheets, experimental works have demonstrated the possibility of controlling the interlayer spacing in GO membranes and use it as water transport channel with salt exclusion up to 97% [74], a performance that is comparable to a typical forward osmosis membrane. On the other hand, GO needs some stabilization strategy (embedded in epoxy, for example) once it can disintegrate in aqueous

solutions [68].

Long before 2D membranes came to the spotlight of research on desalination, membranes composed of CNTs were extensively studied as attractive materials [71]. The investigation of water transport through CNTs led to the discovery of new and exciting properties, such as flow rate enhancement [1], which was seen as a very useful feature for desalination purposes. In 2D materials the high transport rate is associated with their extremely low thickness of just a single atom.

Notwithstanding, the high water transport rate observed in CNTs is a consequence of the smooth hydrophobic inner core, which allows for uninterrupted water molecules passage with negligible adsorption and almost no friction [75]. Indeed, the enhancement flow factor − defined as the ratio between measured flow and the ideal no-slip Poiseuille flow− puts classical hydrodynamic theory in check, once the condition of zero interfacial fluid velocity does not necessarily hold at nanoscopic length scales [58]. This means that while water permeability goes down as we increase the thickness of 2D membranes, it is almost independent of the nanotube length, making CNT membranes still commercially attractive. Secchi et al. [17] have confirmed experimentally fast water transport behavior with nearly frictionless interfaces through carbon nanotubes. Besides these elevated speeds, high aspect ratio and easy functionalization − prerequisite for desalination purposes, avoiding aggregation that harms ion selectivity and water flux− renders CNTs as a widely explored nanomaterial in water purification research.

Among other categories, we could divide CNT-based membranes into two types based on their configurations: freestanding and mixed with polymeric materials [69]. The former can be produced either with vertically aligned nanotubes − where water is forced through inside them − or as buckypaper membranes − in short, a random network of CNTs with large specific surface area. This network is structurally similar to the current commercial thin-film RO membrane composite in which CNTs are mixed with the top layer polymer. Buckypaper CNT membrane poses as an excellent alternative for desalination in distillation technology [76]. In contrast, Baek et al. [77] successfully synthesized a vertically aligned CNT membrane with pore diameters of ~ 4.8 nm and a pore density of 6.8×10^{10} cm^{-2}. They presented improved performance (three times higher flux) compared to typical ultrafiltration (UF) membranes. Additionally, vertically aligned CNT membranes can be obtained from thermal and oxygen-plasma treatments of densified outer-wall CNTs [78]. The advantage of the latter is that pore diameter can be readily varied (e.g., between 7 to 40 nm) through simple mechanical compression. CNT wall membranes obtained in this fashion can deliver water permeability that approaches 30,000 L·m^{-2}·h^{-1}·bar^{-1} and still avoid bacterial adhesion and biofilm formation. As in every other nanoscaled membrane, the experimental challenges here lie on the production of well-defined specific nanotube diameters needed for selectivity purposes, pore size homogeneity, alignment and agglomeration control [62]. MD simulations have suggested that in order to achieve desalination capacity comparable to that of RO membranes the inner diameter of nanotubes should be around 0.6 nm [79], and current state-of-the-art CNT membrane synthesis is not able to meet these requirements. Also, there are concerns about potential nanotoxicity in aquatic environment [70, 80].

CNTs mixed with polymeric materials are well guided to be applied in RO systems. High performance RO CNT/Polyamide membranes can be achieved with CNTs dispersion in typical polymeric matrices [81]. The technique of CNT incorporation into polymers is well-known, and represents an excellent strategy to conceive membranes that are reasonable in terms of water flux (compared to vertically aligned CNTs) but extraordinary in terms of salt permeation, which makes them ideal to improve current RO technology.

Though promising, all of these membrane technologies are still far from reaching the desired

production and commercialization stage. The next generation of desalination membranes is about to face the challenge of keeping the same (high) levels of water permeability, salt rejection, and stability while also becoming industrially scalable. In the meantime, there are several pitfalls to overcome such as chlorine tolerance, fouling/scaling, acid/base, and cleaning. The following section is focused on the gaps and possibilities of MoS_2 and WS_2 as viable alternatives for 2D desalination membranes.

7.5. Research Gaps

a) *Nanopore Opening* – The available synthesis of large-scale MoS_2 and WS_2 single layers by CVD makes them suitable to perform as water desalination 2D membranes. However, nanoporous membranes (Figure 7.2a) require well-defined and distributed openings with pores of $\leq$1 nm radius. This is also true for layered membranes (Figure 7.2b), where superficial nanopores lead to improved filtration and selective ion transport channels. From methods relying on plasma treatment or chemical etching to irradiation with energetic particles, i.e., electrons or ions, there are different ways to open nanopores in 2D membranes. Intrinsic defects in CVD-grown MoS_2 and WS_2 membranes stand as a challenge regarding electron irradiation techniques. While high-energy electrons are able to perforate freestanding MoS_2 and WS_2, single or double vacancies are created during the process [82], limiting their application. Exposing the membrane to a high flux of electrons can also result in an uncontrollable size distribution and pore density. Nevertheless, a combination of methods can be used to achieve the desired scalability. A recent experiment combining focused electron beams with an in situ heating holder was able to drill nanopores in WS_2 bilayers (See Figure 7.4) with precise control over spatial distributions with 5 nm accuracy of patterning and the width of nanowells adjustable by dose-dependent parameters [83]. In contrast to electron beams, we can use ions (or heavy ions) to bombard MoS_2 and WS_2 nanosheets, which involves a wider range of experimental parameters to be explored during the defect creation mechanism. For example, swift heavy ions [84] and highly charged ions [85] have been used to manufacture well-defined openings in freestanding MoS_2. In this way, pores with radii ranging from 0.3 to 3 nm have been created. Some groups have also exploited the electrochemical activity of MoS_2 and WS_2. Debatably, electrochemical reaction (ECR) techniques were used to open well-controlled nanopores in a scalable way [86]. But again, the high density of intrinsic defects naturally occurring in TMDs can represent a drawback for upscaling the method. The large-scale production of 2D MoS_2 and WS_2 to operate as nanoporous membranes depends on the advancement towards improved synthesis and control of nanopore fabrication.

b) *Vacancies* – Due to the imperfect nature of CVD process optimization, intrinsic structural variations such as atomic vacancies and grain boundaries are inherent to CVD-grown 2D MoS_2 and WS_2. In this context, water permeability can be understood in terms of the membrane's intrinsic porosity. Sulfur vacancies of various sizes can yield a large areal density of up to $\sim 10^{13}$ cm^{-2} [22], rendering CVD-grown 2D MoS_2 layers sulfur-deficient in general [87]. Conversely, the areal density of large-sized ($\sim$1 nm) intrinsic sulfur vacancies such as V_{MoS_6} is much smaller than that of small-sized vacancies, for example, V_S of <0.3 nm. This competing situation makes it difficult to experimentally quantify and identify the kind of specific vacancies governing water permeability. Additionally, CVD-grown 2D MoS_2 layers contain a large density of intrinsic "nanopores" present along the grain boundaries formed by individually stitching 2D grains of distinct crystallographic orientation. The size of these nanopores is larger than that of the atomic vacancies within basal planes as they are generally composed of multiple uncoordinated atoms. Grain-boundary nanopores play a very important role in the membrane's

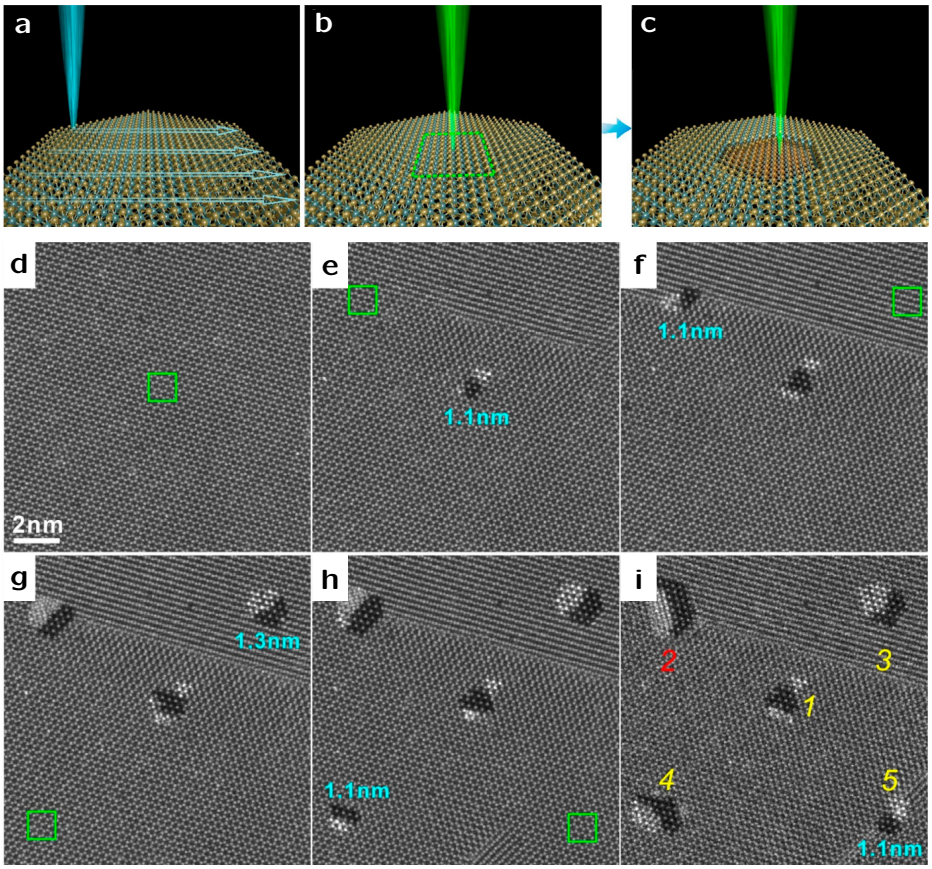

Figure 7.4: Schematic illustration of electron beam used to drill nanopores in bilayer WS_2. Adapted with permission from Chen et al. [83].

permeability, governing both water permeation and ion rejection. The uniformly spaced vdW gaps in the CVD-grown 2D MoS_2 also help the membrane to achieve high ionic sieving capability. In an experimental realization of few-layer 2D MoS_2 membranes Li et al. [12] found the physical sizes of the hydrated ions to be larger than the interlayer vdW MoS_2 gap, which suggests that ion transportation is efficiently impeded. In addition to this geometrical effect, electrostatic interaction of atomic vacancies is considered another major factor governing both water permeation and ionic sieving. Theoretical works have suggested that salt ions encounter significantly high energetic and steric barriers when approaching sulfur vacancies, while water molecules are relatively unaffected [60]. In this case, cations such as Na^+ will experience a high Coulombic barrier due to the positively charged sulfur vacancies, which in turns expose the hydrophilic Mo-rich sites to ignite a process of water attraction and ion repulsion. Indeed, we have identified in our simulations that nanopores with up to ∼1 nm present strong ion rejection rates even at high pressures of ∼100 MPa [13]. Although experimentalists have shown a good control of the naturally occurring defects in CVD growth of TMDs, we still miss a systematic study on the vacancies distribution where their effect, grain boundary and vdW gaps would be properly assessed.

c) *Imaging* – In order to take advantage of all the prominent desalination and adsorption features of MoS_2 and WS_2 membranes, it is very important to establish a precise, reproducible, rapid, and nondestructive method to effectively image nanopores and grain boundaries. This method should be also independent of the membrane composition, doping, and defect reconstruction. Although 2D nanoporous membranes stand as a new class of materials, the character-

ization of solid-state 2D nanostructures is an old, always evolving area of research. Therefore, the long-term knowledge we have built around this technology can be used to access atomic-scale information about nanopore geometry and distribution along the membrane. For instance, we have seen that transmission electron microscopy (TEM) directly resolves atomistic details of defects but requires intensive and disruptive sample preparation [88, 89, 19]. Alternatively, we can use photoluminescence or Raman spectroscopy that provide rapid and nondestructive probes of the electronic and vibrational properties of defective regions. Both techniques often manifest as red- or blue-shifted emission with enhanced or suppressed intensities when compared to the response from a pristine crystal, but it depends on multiple factors that affect local electronic properties such as material composition, doping level, defect passivation, grain boundary geometry, or edge terminations [90, 91]. Nonlinear optical spectroscopy can be highly sensitive to imaging imperfections, but their visualization can exhibit weak background contrast [92] or require the use of chemical solvents [93]. We can alternatively boost image contrast using dark-field (DF) microscopy. By comparing a bright-field linear optical image of a TMD monolayer on quartz and a dark-field linear optical image one can clearly see the edges scattered in dark-field light. However, atomically thin grain boundaries cannot be resolved by either imaging technique, because the in-plane linear dielectric response of TMD monolayers is often isotropic, making the scattered light intensity near grain boundaries indistinguishable. To circumvent this limitation, Carvalho et al. [94] have proposed a dark-field nonlinear characterization technique combining a second harmonic generation microscopy and a spatial filter to further enhance the second harmonic contrast of 1D imperfections in 2D systems (MoS_2 or WS_2), thus allowing detailed large-area spatial mapping of grain boundaries and edges regardless of their local atomic and electronic structures. There is still room for technological innovations in 2D materials characterization. New and improved nanometer-scale imaging techniques are going to rise in decades to come, enabling advancements toward both applications and fundamental 2D materials discoveries.

d) *High Intensive Energy Use* – Nanostructured membranes represent a breakthrough in membrane technology because they allow to shift the trade-off between permeability and salt rejection [62]. It also makes working with less membrane surface than the conventional technology possible. Still, energy consumption at equal operating conditions are very similar to that of traditional salt water RO (limited to a reduction of almost 15% by theoretical calculations based on phenomenological models [95]). In fact, the RO itself is just one stage among others. Because of that, a 15% reduction does not represent much in the overall cost saving. Improvements in pressure bomb technology and pressure recovery systems allowed to reduce energy demand associated with desalination plants over the last decades, but in the end, the costs are ultimately limited by the osmotic pressure in the system. The benefits of using an ultra-permeable membrane are more significant for brackish water RO: a reduction in 46% in energy consumption could in principle be achieved [95]. Besides that, an ultra-permeable membrane opens the window of possibilities to shift the operating conditions in order to optimize the desalination system. Another breakthrough aimed at minimizing energy demand is challenging and necessary to face both the world's water scarcity and climate emergency [96].

e) *Simulations* – Despite the large number of studies, there is still a long way to go when it comes to fully understanding the mechanisms behind 2D membrane desalination. Most of the difficulties are associated with the fact that in the vicinity of an environment as complex as a nanoporous membrane, both water and especially ions can assume completely unpredictable behaviors. For instance, Cohen-Tanugi and Grossman [64] investigated into the role of chemical functional groups bonded to the edges of graphene pores to suggest that commonly occurring hydroxyl groups can roughly double the water flux thanks to their hydrophilic character. It

has been shown that a nozzle-like structure of protein channels and other nanoscale membranes also influence water transport [97]. TMDs such as MoS_2 and WS_2 offer the possibility to craft the pore's edge with Mo(W), S or both, which allows for the design of functional nanopores. Additionally, the fish-bone structure of these TMDs [14] makes it promising as a nozzle-like sub-nanometer pore to be efficiently used in desalination membranes. In their computational study, Heiranian et al. [14] revealed that pore chemistry can significantly impact fluid transport, hence the ion rejection rate. It is important to note, though, that most of the computational results on desalination membranes come from pure classical dynamics. Despite the widespread agreement of these results with experiments, there is still much to advance in the chemical-physical molecular understanding of the processes that lead to higher or lower water fluxes, as well as the mechanisms and interactions between solution and membrane that provide greater efficiency in solute rejection. This can be achieved by using hybrid simulations that consider explicit charge transfer, for example.

f) *T*oxicity − Along with the scalable use of MoS_2 and WS_2 nanomembranes, one of the ultimate challenges is to understand more deeply how these structures are going to affect the environment after release. For instance, nanomaterials may pose a long-term threat if they are persistent and nondegradable [98]. In this regard, both MoS_2 and WS_2 are considered as chemically stable materials against environmental stressors because of the absence of dangling bonds in the terminating S atoms [35]. Particularly the solubility of MoS_2 is low under ambient conditions, which leads to long-term persistence in the environment. On the other hand, this scenario can differ for extreme conditions such as high temperature or strong oxidation, where TMD nanomaterials can be oxidized to different oxides [99]. For instance, the oxidation of MoS_2 nanosheets has been shown to occur in aqueous solutions, leading to soluble, low-toxic oxidation products [100]. The oxidation kinetics depend on factors such as the pH and the crystallographic phase of the TMD.

Toxicity varies depending on preparation methods, but both MoS_2 and WS_2 nanosheets generally show high biocompatibility at concentrations up to $\sim$100 ppm and certain cytotoxicity at high concentrations (a few hundred ppm). For instance, low toxicity of exfoliated, well-dispersed MoS_2 nanosheets was observed, but aggregated samples were found to induce acute lung inflammation in mice [101], raising concerns about their size's effects on the toxicity of these nanosheets. When it comes to toxicity we have good reasons to believe that both MoS_2 and WS_2 nanosheets can perform better than graphene-based nanomaterials [102], but there can be significant differences between those TMDs. Polyethylene glycol (PEG)-coated 2H-MoS_2 nanosheets have shown fast degradation and complete excretion within a month, in marked contrast to WS_2, which presented high levels of concentration in the organs for months [103]. Further degradation experiments indicated that the distinctive in vivo excretion behaviors of TMDs can be attributed to their different chemical properties. Still, the peculiarities involved in degradation and accumulation of each material are yet to be clarified.

7.6. Conclusions and Perspectives

In this chapter we analyzed the unusual 2D film properties of the TMDs MoS_2 and WS_2 with the specific focus for their application as adsorbents and membranes for water purification. The study of 2D materials' transport properties, even though inspired in the enhancement flow observed in carbon nanotubes, has a very different origin. While fast flow in nanotubes is due to friction regardless of tube length, in the case of 2D systems fast liquids transport is associated with their extremely low thickness, and this phenomenon disappears as the layer grows beyond a certain limit. Within single layer surfaces, graphene is the material which not

only has more studies but is also more advanced in production. Nevertheless, TMDs exhibit water permeability two to five orders of magnitude greater than the current technology and 70% better than similar-sized graphene nanopores. These results demonstrate how material's chemistry (especially in nanopores) leads to exotic relationships with water, which is attracted to the inner pore enhancing both water permeation and the rejection of unwanted substances.

The actual nature of the TMD membranes' higher permeability and ion rejection is not clearly understood. In principle, the mix of hydrophobic and hydrophilic edges are important ingredients, yet they do not explain why WS_2 shows water flux two times greater than MoS_2 laminar membranes when both have a very similar charge distribution.

TMD materials can be perfored either by making pores in the perfect material or by building up lamellar structures to employ filtration and adsorption qualities. In both cases impact of defect, pore distribution, and thickness of the stacking layers have to be explored together with the stability and toxicity of the material.

So far, what we have are prominent but diffuse experimental results. With the help of theoretical and computational simulations − in addition to some creativity − it is possible that in the near future both MoS_2 and WS_2 membranes can be used in desalination plants, significantly improving their performance.

Bibliography

[1] M. Majumder, N. Chopra, R. Andrews, and B. J. Hinds, "Enhanced Flow in Carbon Nanotubes," *Nature*, vol. 438, p. 44, 2005.

[2] K. S. Novoselov, A. K. Geim, S. Morozov, D. Jiang, Y. Zhang, S. A. Dubonos, I. Grigorieva, and A. Firsov, "Electric Field Effect in Atomically Thin Carbon Films," *Science*, vol. 306, pp. 666–669, 2004.

[3] K. S. Novoselov, A. K. Geim, S. Morozov, D. Jiang, M. Katsnelson, I. Grigorieva, S. Dubonos, and A. Firsov, "Two-Dimensional Gas of Massless Dirac Fermions in Graphene," *Nature*, vol. 438, pp. 197–200, 2005.

[4] J. Ortiz-Medina, S. Inukai, T. Araki, A. Morelos-Gomez, R. Cruz-Silva, K. Takeuchi, T. Noguchi, T. Kawaguchi, M. Terrones, and M. Endo, "Robust Water Desalination Membranes Against Degradation Using High Loads of Carbon Nanotubes," *Sci. Rep.*, vol. 8, p. 2748, 2018.

[5] S. H. Jamali, T. J. H. Vlugt, and L.-C. Lin, "Atomistic Understanding of Zeolite Nanosheets for Water Desalination," *J. Phys. Chem. C*, vol. 121, pp. 11273–11280, 2017.

[6] J. Dulebohn, P. Ahmadiannamini, T. Wang, S.-S. Kim, T. J. Pinnavaia, and V. V. Tarabara, "Polymer Mesocomposites: Ultrafiltration Membrane Materials with Enhanced Permeability, Selectivity and Fouling Resistance," *J. Membrane Sci.*, vol. 453, pp. 478–488, 2014.

[7] H. Dong, L. Zhao, L. Zhang, H. Chen, C. Gao, and W. S. W. Ho, "High-Flux Reverse Osmosis Membranes Incorporated with NaY Zeolite Nanoparticles for Brackish Water Desalination," *J. Membrane Sci.*, vol. 476, pp. 373–383, 2015.

[8] T. Mouterde, A. Keerthi, A. R. Poggioli, S. A. Dar, A. Siria, A. K. Geim, L. Bocquet, and B. Radha, "Molecular Streaming and its Voltage Control in Angstrom-Scale Channels," *Nature*, vol. 567, pp. 87–90, 2019.

[9] S. Bertolazzi, J. Brivio, and A. Kis, "Stretching and Breaking of Ultrathin MoS_2," *ACS Nano*, vol. 5, pp. 9703–9709, 2011.

[10] R. J. Toh, Z. Sofer, J. Luxa, D. Sedmidubský, and M. Pumera, "3R Phase of MoS_2 and WS_2 Outperforms the Corresponding 2H Phase for Hydrogen Evolution," *Chem. Commun.*, vol. 53, pp. 3054–3057, 2017.

[11] L. Sun, H. Huang, and X. Peng, "Laminar MoS_2 Membranes for Molecule Separation," *Chem. Commun.*, vol. 49, pp. 10718–10720, 2013.

[12] H. Li, T.-J. Ko, M. Lee, H.-S. Chung, S. S. Han, K. H. Oh, A. Sadmani, H. Kang, and Y. Jung, "Experimental Realization of Few Layer Two-Dimensional MoS_2 Membranes of Near Atomic Thickness for High Efficiency Water Desalination," *Nano Lett.*, vol. 19, pp. 5194–5204, 2019.

[13] M. H. Köhler, J. R. Bordin, and M. C. Barbosa, "2D Nanoporous Membrane for Cation Removal from Water: Effects of Ionic Valence, Membrane Hydrophobicity, and Pore Size," *J. Chem. Phys.*, vol. 148, p. 222804, 2018.

[14] M. Heiranian, A. B. Farimani, and N. R. Aluru, "Water Desalination with a Single-Layer MoS_2 Nanopore," *Nat. Commun.*, vol. 6, p. 8616, 2015.

[15] L. Sun, Y. Ying, H. Huang, Z. Song, Y. Mao, Z. Xu, and X. Peng, "Ultrafast Molecule Separation through Layered WS_2 Nanosheet Membranes," *ACS Nano*, vol. 8, pp. 6304–6311, 2014.

[16] K. Liu, Q. Yan, M. Chen, W. Fan, Y. Sun, J. Suh, D. Fu, S. Lee, J. Zhou, S. Tongay, J. Ji, J. B. Neaton, and J. Wu, "Elastic Properties of Chemical-Vapor-Deposited Monolayer MoS_2, WS_2, and Their Bilayer Heterostructures," *Nano Letters*, vol. 14, pp. 5097–5103, 2014.

[17] E. Secchi, S. Marbach, A. Nigues, D. Stein, A. Siria, and L. Bocquet, "Massive Radius-Dependent Flow Slippage in Carbon Nanotubes," *Nature*, vol. 537, pp. 210–213, 2016.

[18] E. R. Hernández, "Molecular Dynamics: From Basic Techniques to Applications (A Molecular Dynamics Primer)," *AIP Conference Proceedings*, vol. 1077, pp. 95–123, 2008.

[19] W. Zhou, X. Zou, S. Najmaei, Z. Liu, Y. Shi, J. Kong, J. Lou, P. M. Ajayan, B. I. Yakobson, and J.-C. Idrobo, "Intrinsic Structural Defects in Monolayer Molybdenum Disulfide," *Nano Letters*, vol. 13, no. 6, pp. 2615–2622, 2013.

[20] S. Najmaei, Z. Liu, W. Zhou, X. Zou, G. Shi, S. Lei, B. I. Yakobson, J.-C. Idrobo, P. M. Ajayan, and J. Lou, "Vapour Phase Growth and Grain Boundary Structure of Molybdenum Disulphide Atomic Layers," *Nat. Mater.*, vol. 12, pp. 754–759, 2013.

[21] H. Y. Jeong, Y. Jin, S. J. Yun, J. Zhao, J. Baik, D. H. Keum, H. S. Lee, and Y. H. Lee, "Heterogeneous Defect Domains in Single-Crystalline Hexagonal WS_2," *Adv. Mater.*, vol. 29, p. 1605043, 2017.

[22] J. Kou, J. Yao, L. Wu, X. Zhou, H. Lu, F. Wu, and J. Fan, "Nanoporous Two-Dimensional MoS_2 Membranes for Fast Saline Solution Purification," *Phys. Chem. Chem. Phys.*, vol. 18, pp. 22210–22216, 2016.

[23] D. Cohen-Tanugi and J. C. Grossman, "Nanoporous Graphene as a Reverse Osmosis Membrane: Recent Insights From Theory and Simulation," *Desalination*, vol. 366, pp. 59–70, 2015.

[24] C. Zhu, H. Li, and S. Meng, "Transport Behavior of Water Molecules Through Two-Dimensional Nanopores," *J. Chem. Phys.*, vol. 141, p. 18C528, 2014.

[25] M. H. Köhler, J. R. Bordin, and M. C. Barbosa, "Ion Flocculation in Water: From Bulk to Nanoporous Membrane Desalination," *J. Mol. Liq.*, vol. 277, pp. 516–521, 2019.

[26] M. D. B. Pérez, A. Nicolai, P. Delarue, V. Meunier, M. Drndic, and P. Senet, "Improved Model of Ionic Transport in 2-D MoS_2 Membranes with Sub-5nm Pores," *Appl. Phys. Lett.*, vol. 114, p. 023107, 2019.

[27] Z. Wang, Q. Tu, S. Zheng, J. J. Urban, S. Li, and B. Mi, "Understanding the Aqueous Stability and Filtration Capability of MoS_2 Membranes," *Nano Lett.*, vol. 17, pp. 7289–7298, 2017.

[28] K. S. Novoselov, A. Mishchenko, A. Carvalho, and A. H. C. Neto, "2D Materials and van der Walls Heterostructures," *Science*, vol. 353, p. aac9439, 2016.

[29] T. Schumann, J. M. J. Lopes, J. M. Wofford, M. H. O. Jr., M. Dubslaff, M.Hanke, U.Jahn, L. Geelhaar, and H. Riechert, "The Impact of Substrate Selection for the Controlled Growth of Graphene by Molecular Beam Epitaxy," *J. Cryst. Growth*, vol. 425, pp. 274–278, 2015.

[30] A. Reina, X. Jia, J. Ho, D. Nezich, H. Son, V. Bulovic, M. S. Dresselhaus, and J. Kong, "Large Area, Few-Layer Graphene Films on Arbitrary Substrates by Chemical Vapor Deposition," *Nano Lett.*, vol. 9, pp. 30–35, 2009.

[31] K. V. Emtsev, A. Bostwick, K. Horn, J. Jobst, G. L. Kellogg, L. Ley, J. L. McChesney, T. Ohta, S. A. Reshanov, J. Röhrl, E. Rotenberg, A. K. Schmid, D. Waldmann, H. B. Weber, and T. Seyller, "Towards Wafer-Size Graphene Layers by Atmospheric Pressure Graphitization of Silicon Carbide," *Nat. Mater.*, vol. 8, pp. 203–207, 2009.

[32] R. K. S. Raman, P. C. Banerjee, D. E. Lobo, H. Gullapalli, M. Sumandasa, A. Kumar, L. Choudhary, R. Tkacz, P. M. Ajayan, and M. Majumder, "Protecting Copper from Electrochemical Degradation by Graphene Coating," *Carbon*, vol. 50, pp. 4040–4045, 2012.

[33] G.-R. Xu, J.-M. Xu, H.-C. Su, X.-Y. Liu, Lu-Li, H.-L. Zhao, H.-J. Feng, and R. Das, "Two-Dimensional (2D) Nanoporous Membranes with Sub-Nanopores in Reverse Osmosis Desalination: Latest Developments and Future Directions," *Desalination*, vol. 451, pp. 18–34, 2019.

[34] X. Li, Z. Zheng, X. Liu, S. Zhao, and S. Liu, "Nanostructured Photoelectrochemical Biosensor for Highly Sensitive Detection of Organophosphorous Pesticides," *Biosens. Bioelectron.*, vol. 64, pp. 1–5, 2015.

[35] M. Chhowalla, H. S. Shin, G. Eda, L.-J. Li, K. P. Loh, and H. Zhang, "The Chemistry of Two Dimensional Layered Transition Metal Dichalcogenide Nanosheets," *Nat. Chem.*, vol. 5, pp. 263–275, 2014.

[36] K. K. Kam and B. A. Parkinson, "Detailed Photocurrent Spectroscopy of the Semiconducting Group VIB Transition Metal Dichalcogenides," *J. Phys. Chem.*, vol. 86, pp. 463–467, 1982.

[37] O. Lopez-Sanchez, D. Lembke, M. Kayci, A. Radenovic, and A. Kis, "Ultrasensitive Photodetectors Based on Monolayer MoS_2," *Nat. Nanotech.*, vol. 8, pp. 497–501, 2013.

[38] S. Tongay, J. Zhou, C. Ataca, K. Lo, T. S. Matthews, J. Li, J. C. Grossman, and J. Wu, "Thermally Driven Crossover from Indirect toward Direct Bandgap in 2D Semiconductors: $MoSe_2$ versus MoS_2," *Nano Lett.*, vol. 12, pp. 5576–5580, 2012.

[39] T. Ohta, A. Bostwick, T. Seyller, K. Horn, and E. Rotenberg, "Controlling the Electronic Structure of Bilayer Graphene," *Science*, vol. 313, pp. 951–954, 2006.

[40] Y. Cao, V. Fatemi, S. Fang, K. Watanabe, T. Taniguchi, E. Kaxiras, and P. Jarillo-Herrero, "Unconventional Superconductivity in Magic-Angle Graphene Superlattices," *Nature*, vol. 556, pp. 43–50, 2018.

[41] M. Buscema, D. J. Groenendijk, S. I. Blanter, G. A. Steele, H. S. J. van der Zant, and A. Castellanos-Gomez, "Fast and Broadband Photoresponse of Few-Layer Black Phosphorus Field-Effect Transistors," *Nano Lett.*, vol. 14, pp. 3347–3352, 2014.

[42] H. Li, J. Wu, X. Huang, G. Lu, J. Yang, X. Lu, Q. Xiong, and H. Zhang, "Rapid and Reliable Thickness Identification of Two-Dimensional Nanosheets Using Optical Microscopy," *ACS Nano*, vol. 7, pp. 10344–10353, 2013.

[43] D. R. Lide, ed., *CRC Handbook of Chemistry and Physics. 81st Edition.* CRC Press: Boca Raton, FL. 2000.

[44] K.-K. Liu, W. Zhang, Y.-H. Lee, Y.-C. Lin, M.-T. Chang, C.-Y. Su, C.-S. Chang, H. Li, Y. Shi, H. Zhang, C.-S. Lai, and L.-J. Li, "Growth of Large-Area and Highly Crystalline MoS_2 Thin Layers on Insulating Substrates," *Nano Lett.*, vol. 12, pp. 1538–1544, 2012.

[45] J. Yoon, W. Park, G.-Y. Bae, Y. Kim, H. S. Jang, Y. Hyun, S. K. Lim, Y. H. Kahng, W.-K. Hong, B. H. Lee, and H. C. Ko, "Highly Flexible and Transparent Multilayer MoS_2 Transistors with Graphene Electrodes," *Small*, vol. 9, pp. 3295–3300, 2013.

[46] G. A. Salvatore, N. Münzenrieder, C. Barraud, L. Petti, C. Zysset, L. Büthe, K. Ensslin, and G. Tröster, "Fabrication and Transfer of Flexible Few-Layers MoS_2 Thin Film Transistors to Any Arbitrary Substrate," *ACS Nano*, vol. 7, pp. 8809–8815, 2013.

[47] B. Kalanyan, W. A. Kimes, R. Beams, S. J. Stranick, E. Garratt, I. Kalish, A. V. Davydov, R. K. Kanjolia, and J. E. Maslar, "Rapid Wafer-Scale Growth of Polycrystalline 2H-MoS2 by Pulsed Metal–Organic Chemical Vapor Deposition," *Chem. Mater.*, vol. 29, pp. 6279–6288, 2017.

[48] H. Zeng, G.-B. Liu, J. Dai, Y. Yan, B. Zhu, R. He, L. Xie, S. Xu, X. Chen, W. Yao, and X. Cui, "Optical Signature of Symmetry Variations and Spin-Valley Coupling in Atomically Thin Tungsten Dichalcogenides," *Sci. Rep.*, vol. 3, p. 1608, 2013.

[49] D. Voiry, H. Yamaguchi, J. Li, R. Silva, D. C. B. Alves, T. Fujita, M. Chen, T. Asefa, V. B. Shenoy, G. Eda, and M. Chhowalla, "Enhanced Catalytic Activity in Strained Chemically Exfoliated WS_2 Nanosheets for Hydrogen Evolution," *Nat. Mater.*, vol. 12, pp. 850–855, 2013.

[50] M. Okada, T. Sawazaki, K. Watanabe, T. Taniguch, H. Hibino, H. Shinohara, and R. Kitaura, "Direct Chemical Vapor Deposition Growth of WS2 Atomic Layers on Hexagonal Boron Nitride," *ACS Nano*, vol. 8, pp. 8273–8277, 2014.

[51] H. Zhu, Y. Wang, J. Xiao, M. Liu, S. Xiong, Z. J. Wong, Z. Ye, Y. Ye, X. Yin, and X. Zhang, "Observation of piezoelectricity in free-standing monolayer MoS_2," *Nat. Nanotech.*, vol. 10, pp. 151–155, 2015.

[52] K. Liu, J. Feng, A. Kis, and A. Radenovic, "Atomically Thin Molybdenum Disulfide Nanopores with High Sensitivity for DNA Translocation," *ACS Nano*, vol. 8, pp. 2504–2511, 2014.

[53] R. Das, C. D. Vecitis, A. Schulze, B. Cao, A. F. Ismail, X. Lu, J. Chen, and S. Ramakrishna, "Recent advances in nanomaterials for water protection and monitoring," *Chem. Soc. Rev.*, vol. 46, pp. 6946–7020, 2017.

[54] N. Peimyoo, J. Shang, W. Yang, Y. Wang, C. Cong, and T. Yu, "Thermal Conductivity Determination of Suspended Mono- and Bilayer WS_2 by Raman Spectroscopy," *Nano Research*, vol. 8, pp. 1210–1221, 2015.

[55] T. Kim, D. Ding, J.-H. Yim, Y.-D. Jho, and A. J. Minnich, "Elastic and Thermal Properties of Free-Standing Molybdenum Disulfide Membranes Measured Using Ultrafast Transient Grating Spectroscopy," *APL Materials*, vol. 5, p. 086105, 2017.

[56] P. Waduge, I. Bilgin, J. Larkin, R. Y. Henley, K. Goodfellow, A. C. Graham, D. C. Bell, N. Vamivakas, S. Kar, and M. Wanunu, "Direct and Scalable Deposition of Atomically Thin Low-Noise MoS_2 Membranes on Apertures," *ACS Nano*, vol. 9, pp. 7352–7359, 2015.

[57] G. Eda, H. Yamaguchi, D. Voiry, T. Fujita, M. Chen, and M. Chhowalla, "Photoluminescence from Chemically Exfoliated MoS_2," *Nano Lett.*, vol. 11, pp. 5111–5116, 2011.

[58] A. J. McGaughey and D. Mattia, "Materials enabling nanofluidic flow enhancement," *MRS Bulletin*, vol. 42, pp. 273–277, 2017.

[59] Z. Wang and B. Mi, "Environmental Applications of 2D Molybdenum Disulfide (MoS_2) Nanosheets," *Environ. Sci. Technol.*, vol. 51, pp. 8229–8244, 2017.

[60] W. Li, Y. Yang, J. K. Weber, G. Zhang, and R. Zhou, "Tunable, Strain-Controlled Nanoporous MoS_2 Filter for Water Desalination," *ACS Nano*, vol. 10, pp. 1829–1835, 2016.

[61] H. Zhang, D. Taymazov, M.-P. Li, Z.-H. Huang, W.-L. Liu, X. Zhang, X.-H. Ma, and Z.-L. Xu, "Construction of MoS_2 composite membranes on ceramic hollow fibers for efficient water desalination," *J. Membrane Sci.*, vol. 59, p. 117369, 2019.

[62] J. R. Werber, C. O. Osuji, and M. Elimelech, "Materials for next-generation desalination and water purification membranes," *Nat. Rev. Mater.*, vol. 1, p. 16018, 2016.

[63] N. Voutchkov, *Desalination Engineering: Planning and Design.* New York: McGraw-Hill, 2013.

[64] D. Cohen-Tanugi and J. C. Grossman, "Water Desalination across Nanoporous Graphene," *Nano Lett.*, vol. 12, pp. 3602–3608, 2012.

[65] F. Risplendi, F. Raffone, L.-C. Lin, J. C. Grossman, and G. Cicero, "Fundamental Insights on Hydration Environment of Boric Acid and Its Role in Separation from Saline Water," *J. Phys. Chem. C*, vol. 124, pp. 1438–1445, 2020.

[66] A. Boretti, S. Al-Zubaidy, M. Vaclavikova, M. Al-Abri, S. Castelletto, and S. Mikhalovsky, "Outlook for Graphene-Based Desalination Membranes," *npj Clean Water*, vol. 1, p. 5, 2018.

[67] S. Homaeigohar and M. Elbahri, "Graphene Membranes for Water Desalination," *NPG Asia Materials*, vol. 9, pp. e427–e427, 2017.

[68] C.-N. Yeh, K. Raidongia, J. Shao, Q.-H. Yang, and J. Huang, "On the Origin of the Stability of Graphene Oxide Membranes in Water," *Nat. Chem.*, vol. 7, pp. 166–170, 2015.

[69] Ihsanullah, "Carbon Nanotube Membranes for Water Purification: Developments, Challenges, and Prospects for the Future," *Sep. Purif. Technol.*, vol. 209, pp. 307–337, 2019.

[70] R. Das, B. F. Leo, and F. Murphy, "The Toxic Truth About Carbon Nanotubes in Water Purification: a Perspective View," *Nanoscale Res. Lett.*, vol. 13, p. 183, 2018.

[71] R. Das, M. E. Ali, S. B. A. Hamid, S. Ramakrishna, and Z. Z. Chowdhury, "Carbon Nanotube Membranes for Water Purification: A Bright Future in Water Desalination," *Desalination*, vol. 336, pp. 97–109, 2014.

[72] S. P. Surwade, S. N. Smirnov, I. V. Vlassiouk, R. R. Unocic, G. M. Veith, S. Dai, and S. M. Mahurin, "Water Desalination Using Nanoporous Single-Layer Graphene," *Nat. Nanotech.*, vol. 10, pp. 459–464, 2015.

[73] K. H. Thebo, X. Qian, Q. Zhang, L. Chen, H.-M. Cheng, and W. Ren, "Highly Stable Graphene-Oxide-Based Membranes with Superior Permeability," *Nat. Commun.*, vol. 9, p. 1486, 2018.

[74] J. Abraham, K. S. Vasu, C. D. Williams, K. Gopinadhan, Y. Su, C. T. Cherian, J. Dix, E. Prestat, S. J. Haigh, I. V. Grigorieva, P. Carbone, A. K. Geim, and R. R. Nair, "Tunable Sieving of Ions Using Graphene Oxide Membranes," *Nat. Nanotech.*, vol. 12, pp. 546–550, 2017.

[75] M. H. Köhler, J. R. Bordin, C. F. de Matos, and M. C. Barbosa, "Water in Nanotubes: The Surface Effect," *Chem. Eng. Sci.*, vol. 203, pp. 54–67, 2019.

[76] L. Dumée, K. Sears, J. Schutz, N. Finn, M. Duke, and S. Gray, "Carbon Nanotube Based Composite Membranes for Water Desalination by Membrane Distillation," *Desalination and Water Treatment*, vol. 17, pp. 72–79, 2010.

[77] Y. Baek, C. Kim, D. K. Seo, T. Kim, J. S. Lee, Y. H. Kim, K. H. Ahn, S. S. Bae, S. C. Lee, J. Lim, K. Lee, and J. Yoon, "High Performance and Antifouling Vertically Aligned Carbon Nanotube Membrane for Water Purification," *J. Membrane Sci.*, vol. 460, pp. 171–177, 2014.

[78] B. Lee, Y. Baek, M. Lee, D. H. Jeong, H. H. Lee, J. Yoon, and Y. H. Kim, "A Carbon Nanotube Wall Membrane for Water Treatment," *Nat. Commun.*, vol. 6, p. 7109, 2015.

[79] C. H. Ahn, Y. Baek, C. Lee, S. O. Kim, S. Kim, S. Lee, S.-H. Kim, S. S. Bae, J. Park, and J. Yoon, "Carbon Nanotube-Based Membranes: Fabrication and Application to Desalination," *J. Ind. Eng. Chem.*, vol. 18, pp. 1551–1559, 2012.

[80] A. P. Francis and T. Devasena, "Toxicity of Carbon Nanotubes: A Review," *Toxicology and Industrial Health*, vol. 34, pp. 200–210, 2018.

[81] H. J. Kim, K. Choi, Y. Baek, D.-G. Kim, J. Shim, J. Yoon, and J.-C. Lee, "High-Performance Reverse Osmosis CNT/Polyamide Nanocomposite Membrane by Controlled Interfacial Interactions," *ACS Appl. Mater. Interfaces*, vol. 6, pp. 2819–2829, 2014.

[82] H.-P. Komsa, J. Kotakoski, S. Kurasch, O. Lehtinen, U. Kaiser, and A. V. Krasheninnikov, "Two-Dimensional Transition Metal Dichalcogenides under Electron Irradiation: Defect Production and Doping," *Phys. Rev. Lett.*, vol. 109, p. 035503, 2012.

[83] J. Chen, G. H. Ryu, Q. Zhang, Y. Wen, K.-L. Tai, Y. Lu, and J. H. Warner, "Spatially Controlled Fabrication and Mechanisms of Atomically Thin Nanowell Patterns in Bilayer WS_2 Using in Situ High Temperature Electron Microscopy," *ACS Nano*, vol. 13, pp. 14486–14499, 2019.

[84] L. Madauß, O. Ochedowski, H. Lebius, B. Ban-d'Etat, C. H. Naylor, A. T. C. Johnson, J. Kotakoski, and M. Schleberger, "Defect Engineering of Single- and Few-Layer MoS_2 by Swift Heavy Ion Irradiation," *2D Materials*, vol. 4, p. 015034, 2016.

[85] R. Kozubek, M. Tripathi, M. Ghorbani-Asl, S. Kretschmer, L. Madauß, E. Pollmann, M. O'Brien, N. McEvoy, U. Ludacka, T. Susi, G. S. Duesberg, R. A. Wilhelm, A. V. Krasheninnikov, J. Kotakoski, and M. Schleberger, "Perforating Freestanding Molybdenum Disulfide Monolayers with Highly Charged Ions," *J. Phys. Chem. Lett.*, vol. 10, pp. 904–910, 2019.

[86] J. Feng, K. Liu, M. Graf, M. Lihter, R. D. Bulushev, D. Dumcenco, D. T. L. Alexander, D. Krasnozhon, T. Vuletic, A. Kis, and A. Radenovic, "Electrochemical reaction in single layer MoS_2: Nanopores opened atom by atom," *Nano Lett.*, vol. 15, pp. 3431–3438, 2015.

[87] J. Hong, Z. Hu, M. Probert, K. Li, D. Lv, X. Yang, L. Gu, N. Mao, Q. Feng, L. Xie, J. Zhang, D. Wu, Z. Zhang, C. Jin, W. Ji, X. Zhang, J. Yuan, and Z. Zhang, "Exploring Atomic Defects in Molybdenum Disulphide Monolayers," *Nat. Commun.*, vol. 6, p. 6293, 2015.

[88] O. Lehtinen, H.-P. Komsa, A. Pulkin, M. B. Whitwick, M.-W. Chen, T. Lehnert, M. J. Mohn, O. V. Yazyev, A. Kis, U. Kaiser, and A. V. Krasheninnikov, "Atomic Scale Microstructure and Properties of Se-Deficient Two-Dimensional $MoSe_2$," *ACS Nano*, vol. 9, pp. 3274–3283, 2015.

[89] A. Azizi, X. Zou, P. Ercius, Z. Zhang, A. L. Elías, N. Perea-López, G. Stone, M. Terrones, B. I. Yakobson, and N. Alem, "Dislocation Motion and Grain Boundary Migration in Two-Dimensional Tungsten Disulphide," *Nat.Commun.*, vol. 5, p. 4867, 2014.

[90] H. Nan, Z. Wang, W. Wang, Z. Liang, Y. Lu, Q. Chen, D. He, P. Tan, F. Miao, X. Wang, J. Wang, and Z. Ni, "Strong Photoluminescence Enhancement of MoS_2 through Defect Engineering and Oxygen Bonding," *ACS Nano*, vol. 8, pp. 5738–5745, 2014.

[91] K.-I. Lin, Y.-H. Ho, S.-B. Liu, J.-J. Ciou, B.-T. Huang, C. Chen, H.-C. Chang, C.-L. Tu, and C.-H. Chen, "Atom-Dependent Edge-Enhanced Second-Harmonic Generation on MoS_2 Monolayers," *Nano Lett.*, vol. 18, pp. 793–797, 2018.

[92] X. Yin, Z. Ye, D. A. Chenet, Y. Ye, K. O'Brien, J. C. Hone, and X. Zhang, "Edge Nonlinear Optics on a MoS_2 Atomic Monolayer," *Science*, vol. 344, pp. 488–490, 2014.

[93] L. Karvonen, A. Säynätjoki, M. J. Huttunen, A. Autere, B. Amirsolaimani, S. Li, R. A. Norwood, N. Peyghambarian, H. Lipsanen, G. Eda, K. Kieu, and Z. Sun, "Rapid Visualization of Grain Boundaries in Monolayer MoS_2 by Multiphoton Microscopy," *Nat. Commun.*, vol. 8, p. 15714, 2017.

[94] B. R. Carvalho, Y. Wang, K. Fujisawa, T. Zhang, E. Kahn, I. Bilgin, P. M. Ajayan, A. M. de Paula, M. A. Pimenta, S. Kar, V. H. Crespi, M. Terrones, and L. M. Malard, "Nonlinear Dark-Field Imaging of One-Dimensional Defects in Monolayer Dichalcogenides," *Nano Lett.*, vol. 20, pp. 284–291, 2020.

[95] D. Cohen-Tanugi, R. K. McGovern, S. H. Dave, J. H. Lienhard, and J. C. Grossman, "Quantifying the Potential of Ultra-Permeable Membranes for Water Desalination," *Energy Environ. Sci.*, vol. 7, pp. 1134–1141, 2014.

[96] WWAP and UNESCO, *The United Nations World Water Development Report 2019: Leaving no One Behind.* 2019.

[97] S. Gravelle, L. Joly, F. Detcheverry, C. Ybert, C. Cottin-Bizonne, and L. Bocquet, "Optimizing Water Permeability through the Hourglass Shape of Aquaporins," *Proc. Natl. Acad. Sci. U.S.A.*, vol. 110, pp. 16367–16372, 2013.

[98] Z. Wang, W. Zhu, Y. Qiu, X. Yi, A. von dem Bussche, A. Kane, H. Gao, K. Koski, and R. Hurt, "Biological and Environmental Interactions of Emerging Two-Dimensional Nanomaterials," *Chem. Soc. Rev.*, vol. 45, pp. 1750–1780, 2016.

[99] J. Gao, B. Li, J. Tan, P. Chow, T.-M. Lu, and N. Koratkar, "Aging of Transition Metal Dichalcogenide Monolayers," *ACS Nano*, vol. 10, pp. 2628–2635, 2016.

[100] Z. Wang, A. von dem Bussche, Y. Qiu, T. M. Valentin, K. Gion, A. B. Kane, and R. H. Hurt, "Chemical Dissolution Pathways of MoS_2 Nanosheets in Biological and Environmental Media," *Environ. Sci. Technol.*, vol. 50, pp. 7208–7217, 2016.

[101] X. Wang, N. D. Mansukhani, L. M. Guiney, Z. Ji, C. H. Chang, M. Wang, Y.-P. Liao, T.-B. Song, B. Sun, R. Li, T. Xia, M. C. Hersam, and A. E. Nel, "Differences in the Toxicological Potential of 2D versus Aggregated Molybdenum Disulfide in the Lung," *Small*, vol. 11, pp. 5079–5087, 2015.

[102] W. Z. Teo, E. L. K. Chng, Z. Sofer, and M. Pumera, "Cytotoxicity of Exfoliated Transition-Metal Dichalcogenides (MoS_2, WS_2, and WSe_2) is Lower Than That of Graphene and its Analogues," *Chem. Eur. J.*, vol. 20, pp. 9627–9632, 2014.

[103] J. Hao, G. Song, T. Liu, X. Yi, K. Yang, L. Cheng, and Z. Liu, "In Vivo Long-Term Biodistribution, Excretion, and Toxicology of PEGylated Transition-Metal Dichalcogenides MS_2 (M = Mo, W, Ti) Nanosheets," *Adv. Science*, vol. 4, p. 1600160, 2017.